Swinburne Research Bank

http://researchbank.swinburne.edu.au

Galaxy threshing and the origin of ultra-compact dwarf galaxies in the Fornax cluster

K. Bekki,[1] W. J. Couch[1] M. J. Drinkwater[2], and Y. Shioya[3]

[1] *School of Physics, University of New South Wales, Sydney 2052, NSW, Australia*
[2] *Department of Physics, University of Queensland, Queensland 4072, Australia*
[3] *Astronomical Institute, Tohoku University, Sendai, 980-8578, Japan*

arXiv:astro-ph/0308243v1 14 Aug 2003

ABSTRACT

A recent all-object spectroscopic survey centred on the Fornax cluster of galaxies, has discovered a population of sub-luminous and extremely compact members, called "ultra-compact dwarf" (UCD) galaxies. In order to clarify the origin of these objects, we have used self-consistent numerical simulations to study the dynamical evolution a nucleated dwarf galaxy would undergo if orbiting the center of the Fornax cluster and suffering from its strong tidal gravitational field. We find that the outer stellar components of a nucleated dwarf are removed by the strong tidal field of the cluster, whereas the nucleus manages to survive as a result of its initially compact nature. The developed naked nucleus is found to have physical properties (e.g., size and mass) similar to those observed for UCDs. We also find that although this formation process does not have a strong dependence on the initial total luminosity of the nucleated dwarf, it does depend on the radial density profile of the dark halo in the sense that UCDs are less likely to be formed from dwarfs embedded in dark matter halos with central 'cuspy' density profiles. Our simulations also suggest that very massive and compact stellar systems can be rapidly and efficiently formed in the central regions of dwarfs through the merging of smaller star clusters. We provide some theoretical predictions on the total number and radial number density profile of UCDs in a cluster and their dependences on cluster masses.

Key words: dwarf — galaxies: clusters: general — galaxies: elliptical and lenticular, cD – galaxies: formation – galaxies: interactions

1 INTRODUCTION

The population of low-luminosity, low surface brightness dwarf elliptical and irregular galaxies are thought to have a key role in the context of galaxy formation and evolution. This is not only because in the hierarchical clustering scenario these small galaxies merge to form more massive galaxies, but also because their observed physical properties place strong constraints on theoretical models of galaxy formation and evolution (e.g., Ferguson & Binggeli 1994; Mateo 1998; Grebel 1998). Examples of the latter include the scaling relation (Kormendy 1977; Ferguson & Binggeli 1994), the luminosity function (Binggeli, Sandage, & Tammann 1985; Sandage, Binggeli, & Tammann 1985), the presence of nuclear structures (Binggeli & Cameron 1991), and rotation-curve profiles (Moore 1994), all of which have been extensively discussed for assessing the viability of any theory of galaxy formation and evolution.

In contrast to this ubiquitous dwarf galaxy population,

the red compact elliptical galaxies (cE) such as M32 are very rarely observed and are preferentially located in close proximity to giant galaxies (e.g., Nieto & Prugniel 1987). Only recently, Forbes et al. (2002) have discovered another clear example of an M32-like compact spheroidal system very close to an M31-like spiral galaxy, in the image of UGC 10214 taken by Advanced Camera for Surveys (*ACS*) on board the Hubble Space Telescope (*HST*). The origin of the high surface brightness and radially-limited luminosity profiles of such objects has been discussed by several authors mostly in the context of the tidal effects of the massive galaxies they lie close to (King 1962; Faber 1973; Nieto & Prugniel 1987; Burkert 1994; Bekki et al. 2001a). It is, however, still controversial how such compact density profiles are formed via the tidal gravitational forces of massive galaxies.

A new type of sub-luminous and extremely compact "dwarf galaxy" has recently been discovered in an "all-object" spectroscopic survey centred on the Fornax cluster of galaxies (Drinkwater et al. 2000a, b). While objects with

this type of *morphology* have been observed before – the bright compact objects discovered by Hilker et al. 1999 – and the very luminous globular clusters around cD galaxies (Harris, Pritchet, & McClure 1995) – in this particular case they have been found to be members of the Fornax cluster, have intrinsic sizes of only $\sim 100\,\mathrm{pc}$, and have absolute $B-$band magnitudes ranging from -13 to -11 mag. Hence Drinkwater et al. have named them "ultra-compact dwarf" (UCD) galaxies. Importantly, the luminosities of UCDs are intermediate between those of globular clusters and small dwarf galaxies and are similar to those of the bright end of the luminosity function of the nuclei of nucleated dwarf ellipticals (e.g., Lotz et al. 2001). Moreover, they are observed to be within 30 arcmin of the central dominant galaxy in Fornax, NGC 1399, and are distributed as large radii as this galaxy's globular cluster system (extending out to a radius of 100 kpc at least; Dirsch et al. 2003). Owing to the lack of ultra high-resolution imaging and high-dispersion spectroscopy of the UCDs, it was highly uncertain at the time of their discovery whether they are super-massive star clusters (intracluster globular clusters or tidally stripped nuclei of dwarf galaxies) or really a new type of low-luminosity compact elliptical dwarf ("M32-type") galaxy (Drinkwater et al. 2000b).

However, Drinkwater et al. (2003; hereafter D03) recently obtained high-resolution imaging of the UCDs in Fornax with the Space Telescope Imaging Spectrograph (STIS) on HST and found that their radial density profiles (with one exception) can be well fitted by both King model and de Vaucouleurs $R^{1/4}$ profiles. The effective radii measured for the UCDs were in the $10 - 30$ pc range, which is larger than the typical core radius of a globular cluster ($\sim 6\,\mathrm{pc}$) and smaller than the scale length of the most compact normal dwarf galaxy in the Virgo cluster (~ 160 pc). D03 also obtained high-resolution spectra of UCDs using the Very Large Telescope UV Echelle Spectrograph and the Keck Telescope Echelle Spectrograph. These were used to measure internal velocity dispersions and, in turn, mass-to-light (M/L) ratios for the UCDs. These ranged from 24 to 37 km s^{-1} and 2 to 4 $M/L_\odot$, respectively. These observations suggest that UCDs are different from normal dwarf galaxies in size and from GCs in velocity dispersion and M/L: UCDs are thus observed to be really a new class of galactic object!

The importance of the tidal field of more massive galaxies in forming globular clusters (and even objects that are an order of magnitude brighter than globular clusters) from nucleated dwarf galaxies has already been discussed by several authors (e.g., Zinnecker et al. 1988; Freeman 1993; Bassino et al. 1994). Bassino et al. (1994) first demonstrated that very massive globular clusters can originate from nuclei of nucleated dwarf galaxies around more massive galaxies owing to the tidal stripping of the stellar envelope of the dwarfs. Using more realistic numerical simulations, Bekki et al. (2001b) proposed the "galaxy threshing scenario" in which the global tidal field of the Fornax cluster efficiently strips the outer stellar envelopes of the more massive nucleated dwarf galaxies ($\mathrm{M_d} \sim 10^8\,\mathrm{M_\odot}$) as they orbit NGC 1399. This was shown to transform them into compact systems whose luminosity was consistent with that of the UCDs. This previous study, however, did not discuss structural and kinematical properties (e.g., radial density profile, velocity dispersion, and mass-to-light-ratio) of which there are now

measurements from HST and the large ground-based telescopes (D03).

The purpose of this paper is to numerically investigate the threshing scenario in a more comprehensive and self-consistent manner and to specifically address and compare these structural and kinematical properties. Based on a fully self-consistent dynamical model of dE,Ns embedded in massive dark matter halos, we investigate the following issues: (i) how the global tidal field of the Fornax cluster strips the dark matter halos, the stellar envelopes, and the nuclei of dE,Ns with different luminosites, (ii) whether the structural properties of the dark matter halos of dE'Ns are important for the effectiveness of the threshing process, (iii) whether galaxy threshing can transform nucelated dwarf spirals into UCDs, (iv) whether the galaxy threshing scenario can explain the relationship between velocity dispersion and absolute magnitude observed for UCDs, and (v) what the threshing scenario predicts for the total number and the radial number distribution of UCDs in a cluster and their dependence on cluster mass. We also discuss a possible physical relationship between UCDs, the globular cluster ωCen, and the compact elliptical galaxy M32 and a formation mechanism for the nuclei of dE,Ns.

The plan of the paper is as follows: In the next section, we describe our numerical model for the dynamical evolution of dE,Ns in the Fornax cluster. In §3, we present our numerical results on the structural and kinematical properties of UCDs formed by galaxy threshing and compare these with recent observational results. In §4, we discuss the environmental dependences of UCD properties, the possible formation of the giant globular cluster ωCen via threshing, and the formation of galactic nuclei in dwarfs via merging of globular clusters. We summarise our conclusions in §5.

2   MODEL DETAILS

2.1   Cluster mass profile

In order to model, numerically, the dynamical evolution of nucleated dwarf galaxies as they orbit the centre of the Fornax cluster, we consider them to be collisionless stellar systems with a mass and size similar to that observed for the dE,N types. We assume that the gravitational field of the cluster's dark matter halo has the strongest influence on the dynamical evolution of dE,Ns. Accordingly, we model only the cluster tidal field and do not include any tidal effects from other cluster member galaxies in the present simulations. Also cluster potential is assumed to be time-indepedent, which is not so consistent with recent high-resolution numerical simulations of cluster galxies formation within the CDM models (e.g., Ghigna et al. 1998). Although our simulations are thus idealized in some aspects, we believe that our model still contains the essential ingredients that govern the dynamical evolution of dE,Ns in the Fornax cluster.

To give our model a realistic radial density profile for the dark matter halo of the cluster, we base it on both the X-ray observations of Jones et al. (1997) and the predictions from the standard cold dark matter cosmogony (Navarro, Frenk, & White 1996, hereafter NFW). The NFW profile is described as:

$$\rho(r) = \frac{\rho_0}{(r/r_{\rm s})(1 + r/r_{\rm s})^2}, \tag{1}$$

where r, ρ_0, and $r_{\rm s}$ are the distance from the center of the cluster, the central density, and the scale-length of the dark halo, respectively. The adopted NFW model has a total mass of $7.0 \times 10^{13} {\rm M}_\odot$ (within the virial radius) and $r_{\rm s}$ of 83 kpc. This model is based on the NFW model with a "c" parameter of 12.8. The adopted set of parameters is consistent with the X-ray observations of Jones et al. (1997) and the mass estimation of the Fornax cluster derived from kinematics of the cluster galaxies by Drinkwater et al. (2001). This cluster model is referred to as "the Fornax profile" and labeled as "FO".

To determine the dependences of the galaxy threshing processes on cluster mass and size, we have also investigated the dynamical evolution of dE,Ns for other model clusters. In particular, we present the results for models with $M_{\rm cl} = 5.0 \times 10^{14} {\rm M}_\odot$ and $r_{\rm s} = 226$ kpc, as well as $M_{\rm cl} = 3.0 \times 10^{13} {\rm M}_\odot$ and $r_{\rm s} = 83$ kpc. The more massive model corresponds to the Virgo cluster, and accordingly it is referred to as "VO" model; the less massive model corresponds to the Local Group and is referred to as the "LG" model. All of the parameters for these are chosen from the values listed in Table of NFW (e.g, model 3 and 15).

2.2 Nucleated dwarf ellipticals

A dE,N is modelled as a fully self-gravitating system and assumed to consist of a dark matter halo, a stellar component, and a nucleus. We accordingly do not include any gaseous components in the present models. For convenience, the stellar component (i.e., the main baryonic component) is referred to as either the "envelope" or the "stellar envelope" so that we can distinguish this component from the stellar nucleus. The density profile of the dark matter halo of the dE,N is represented by that proposed by Salucci & Burkert (2000):

$$\rho_{\rm dm}(r) = \frac{\rho_{dm,0}}{(r + a_{\rm dm})(r^2 + a_{\rm dm})^2}, \tag{2}$$

where $\rho_{dm,0}$ and $a_{\rm dm}$ are the central dark matter density and the core (scale) radius, respectively. For convenience, we hereafter call this profile the "SB" profile (or model). The main difference between the SB profile and the NFW profile is that the former has a large dark matter core. We choose the SB profile rather than the NFW profile, because the observed kinematics of dwarf galaxies are inconsistent with the cuspy dark matter profiles predicted by the CDM model (e.g., Moore 1994; Burkert 1995). For the SB profile, the dark matter core parameters, $\rho_{dm,0}$, $a_{\rm dm}$, and M_0 (where M_0 is the total dark matter mass within $a_{\rm dm}$) are not free parameters, and clear correlations are observed between them (Burkert 1995):

$$M_0 = 4.3 \times 10^7 (\frac{a_{\rm dm}}{\rm kpc})^{7/3} M_\odot. \tag{3}$$

All dark matter particles are distributed within $5a_{\rm dm}$.

Equations (2) and (3) predict that $a_{\rm dm}$ is ~ 3.5 times larger than the typical scale length (~ 800 pc) observed for dE,Ns, with $M_{\rm B} = -16$ mag and $M/L_{\rm B} = 10$ (Ferguson & Binggeli 1994). This large core radius is a favorable condition for galaxy threshing to act on dE,Ns, as is described

later. Since the dE,N model with $M_{\rm B} = -16$ mag is the most extensively investigated, the $a_{\rm dm}$ of this model is hereafter referred to as $a_{\rm dm,0}$. In order to clarify the importance of the dark matter halo profiles of dE,Ns in the galaxy threshing process, we also investigate models with NFW dark matter profiles with a scale radius of $a_{\rm s}$. For the scale radius of a cluster's dark matter halo to be distinguished from that of a galactic dark matter halo, we here use $a_{\rm s}$ rather than the original definition of $r_{\rm s}$. Since there are no results on the scale radius $a_{\rm s}$ for dark matter halos of typical dwarfs (with $M_{\rm dm} \sim 10^9 M_\odot$) in NFW, direct comparison between $a_{\rm s}$ and $a_{\rm dm}$ for a given total mass of a dark matter halo is not possible. If we assume that the central density of the dark matter halo with $M_{\rm dm} = 4 \times 10^9 M_\odot$ (corresponding to the above $M_{\rm B} = -16$ mag dE,N model) is the same as that of the halo with $M_{\rm dm} = 3.2 \times 10^{11} M_\odot$ (corresponding to model 1 in Table of NFW), $a_{\rm s}$ is estimated to be $\sim 0.7a_{\rm dm}$. The CDM model predicts that dark matter halos with lower masses can show higher central densities (NFW), and $a_{\rm s}/a_{\rm dm}$ can be smaller than 1 for a given dE,N dark matter halo mass. Guided by this simple estimation, we investigate the models with $a_{\rm s} = a_{\rm dm,0}$, $0.5a_{\rm dm,0}$, and $0.25a_{\rm dm,0}$.

The mass (luminosity) and the scale length of the stellar envelope in a dE,N is modelled according to the observed scaling relation of Ferguson & Binggeli (1994):

$$\log r_0 [{\rm pc}] = -0.2M_{\rm B} - 0.3 \tag{4}$$

for bright dwarfs ($M_{\rm B} < -16$) and

$$\log r_0 [{\rm pc}] = -0.02M_{\rm B} + 2.6 \tag{5}$$

for faint dwarfs ($M_{\rm B} \geq -16$), where r_0 and $M_{\rm B}$ are the scale length of the exponential profile and the absolute $B-$band magnitude, respectively. The projected density of the envelope with $M_{\rm B}$ and the total mass of $M_{\rm dw}$ is represented by an exponential profile with a scale length $a_{\rm dw}$ that is exactly the same as r_0 in the above equation for the value of $M_{\rm B}$. The ratio of the total mass of the envelope to the total luminosity of the envelope is set to be 2. The projected density profile of the nucleus with mass $M_{\rm n}$ is represented by a King model (King 1964) with a core radius of $a_{\rm n}$ and a central concentration parameter c of 1.0.

We estimate the velocities of both the dark matter halo particles and the stellar envelope particles from the gravitational potential at the positions where they are located. In detail, we first calculate the one-dimensional isotropic dispersion according to the (local) virial theorem:

$$\sigma^2(r) = -\frac{U(r)}{3}, \tag{6}$$

where $U(r)$ is the gravitational potential at the position r. We then allocate a velocity to each collisionless particle (dark matter halo and stellar particles) so that the distribution of velocities of these particles have a Gaussian form with a dispersion equal to $\sigma^2(r)$. We consider that the nucleus is strongly self-gravitating and thus the one-dimensional isotropic dispersion at a given radius in the nucleus is determined solely by the gravitational potential of the nucleus (i.e., the outer dark matter halo and the envelope do not contribute significantly to the potential at the very center of the dE,N). This is consistent with recent simulation results (Oh & Lin 2000), which suggest that the relatively low central velocity dispersion of a dE,N can be
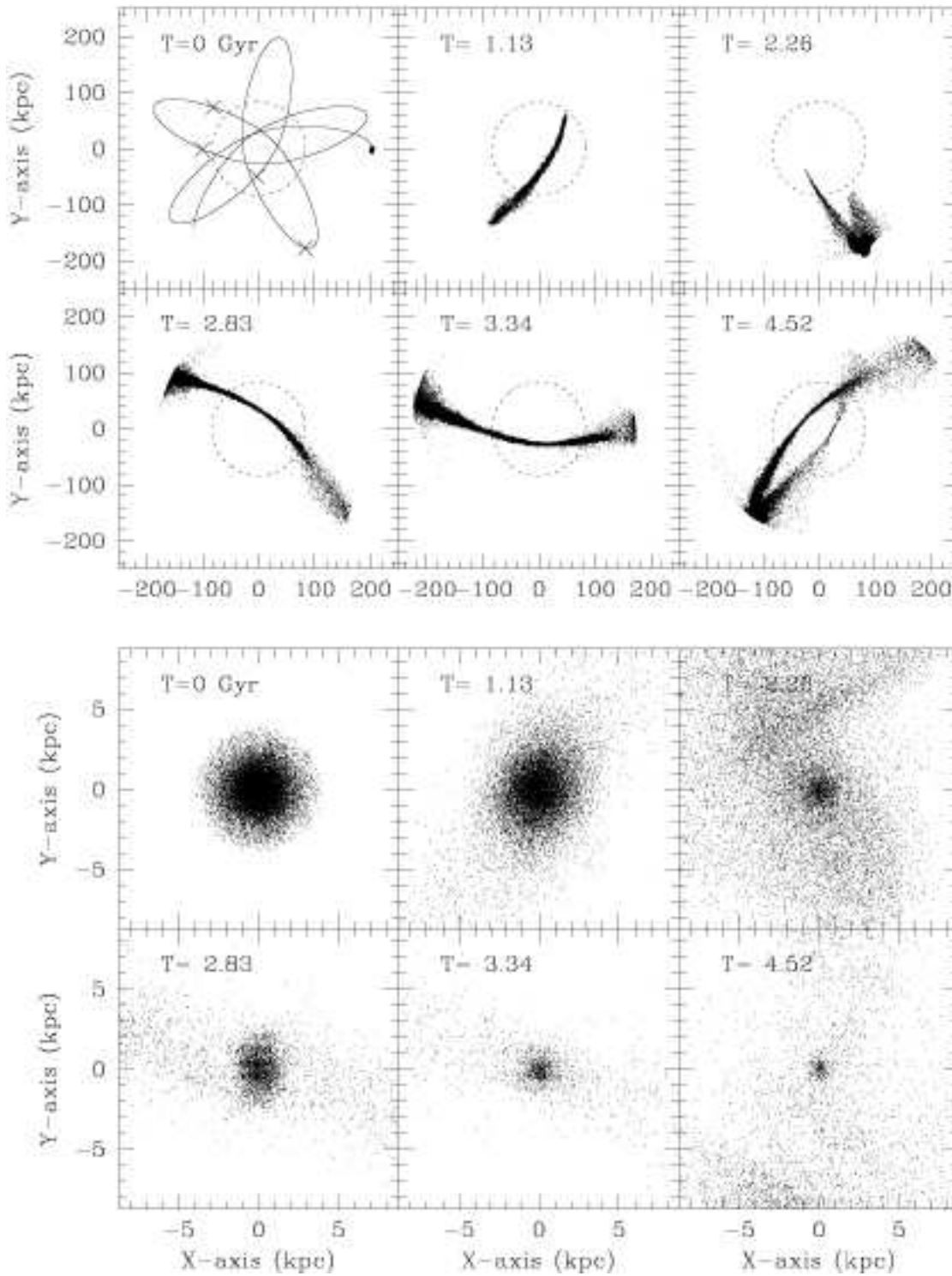
Figure 1. Morphological evolution of the stellar components (the stellar envelope and the nucleus) of the dE,N projected onto the x-y plane for the fiducial model (FO1). The time T (in units of Gyr) indicated in the upper left corner of each frame represents the time that has elapsed since the simulation starts. Each frame is 500 kpc on a side in the upper six panels and 17.5 kpc on a side in the lower panels. The orbital evolution of the dE,N at 4.5 Gyr is indicated by the solid line in the upper left panel in the upper six panels. The location of the nucleus of the dwarf is indicated by crosses for $T = 1.13$, 2.26, 2.83, and 3.34 Gyr. The scale radius of the adopted NFW model for the dark matter halo distribution of the Fornax cluster mass profile is indicated by a dotted circle in each of the upper six panels.

due to the self-gravitating nucleus formed by the merging of nuclear star clusters. The method of determining the value of the velocity dispersion from the gravitational potential at a given radius for the nucleus is the same as that for the dark matter and the stellar envelope.

For all dE,N models, the mass-to-light-ratio in the $B-$band (M/L_B) is set to be 10 (thus $M_{dm}/M_{dw} = 5$). Therefore, if we choose M_B for a dE,N model, then its values of M_{dm}, a_{dm}, and a_{dw} are automatically determined from equations (3) and (4). The remaining parameters of the dE,N model are a_n/a_{dw} and M_n/M_{dw}. These range from 0.02 to 0.2 for a_n/a_{dw} and from 0.02 to 0.2 for M_n/M_{dw}, and we show the results of the models that have particularly important implications for UCD formation via galaxy threshing. The adopted parameter values are all consistent with those observed in dE,Ns (e.g., Binggeli & Cameron 1991; Ferguson & Binggeli 1994).

The adopted value of 10 for M/L_B is consistent with observational results of *some* dEs with well know kinematical properties. Mateo et al. (1991) estimated M/L_B as 12±4 for the Fornax dwarf galaxy based on the precisely determined radial velocities of 44 individual stars of the dwarf. The M/L estimated from radial velocity dispersion in dwarf spheroidal galaxies in the Local group is summarized in van den Bergh (2000): $6-13$ for the Leo I, ~ 23 for the Carina dwarf, 13±6 for the Sculptor, ~ 90 for the Draco, ~ 12 for the Leo II, and ~ 50 for the Sextans. Accordingly, the adopted value of 10 in the present simulations is reasonably consistent with observations of the Local group dwarfs except the Draco and the Sextans with the unusually large M/L.

2.3 High– and low-surface brightness spirals

We also investigate the threshing processes for nucleated low-luminosity spiral galaxies ($M_B = -16$ mag) dominated by dark matter halos in order to investigate whether UCD formation processes depend on the morphological properties of their hosts. Such galaxies are modelled by assuming they have an exponential stellar disk (with a radial scale length of a_{disc} and a vertical scale length of $0.2a_{disc}$) which is embedded in a dark matter halo. The latter is represented by an SB profile with a core radius a_{dm}, and a total mass 10 times larger than the stellar disk. The value of a_{dm}/a_{disc} is set to be 6.0 for the models, which ensures that the model galaxies' rotation curves are of similar shape to that of the Galaxy. In addition to the rotational velocity due to the gravitational field of the disk and halo components, initial radial and azimuthal velocity dispersions are assigned to the disk component according to the epicyclic theory of Binney & Tremaine (1987) with a Toomre parameter value of $Q = 1.5$. The vertical velocity dispersion at a given radius is set to be half the radial velocity dispersion at that point, consistent with that observed in the Milky Way (e.g., Wielen 1977).

We present the results for models with $M_B = -16.0$ and central surface brightnesses of $\mu_0 = 22$ mag arcsec^{-2} in $B-$band (hereafter referred to as the "HSB" model), 24 ("LSBI") and 26 mag arcsec^{-2} ("LSBII"). For all spiral models with $M_B = -16.0$, the physical parameters of the nuclei are the same as those adopted in the fiducial dE,N (FO1) model described later. The adopted value of 10 for the mass-to-light-ratio is reasonable for simulations of LSBs (e.g., Mi-

hos et al. 1997). The gaseous component is not included in the HSB and LSB models, because we consider that low density gas in these galaxies can be quickly stripped from them because of ram pressure stripping in cluster environments.

2.4 Orbits

The orbit of our model dE,N (and a dwarf spiral) is assumed to be influenced only by the gravitational potential resulting from the dark halo component of the Fornax cluster. Since the adopted cluster potential is spherically symmetric (not triaxial), the orbit of the dE,N forms a rosette within a plane. This orbital plane defines the x-y plane in all our models.

The center of the cluster is always set to be $(x,y,z) = (0,0,0)$ whereas the initial position of the dE,N is set to be $(x,y,z) = (R_{ini}, 0, 0)$. The initial velocity of the dE,N (v_x,v_y,v_z) is set to be $(0, f_vV_c, 0)$, where f_v and V_c are the parameters controlling the orbital eccentricity (i.e, the larger f_v is, the more circular the orbit becomes) and the circular velocity of the cluster at $R = R_{ini}$, respectively.

We investigate three representative values of f_v: 0.25, 0.5, and 1, the corresponding orbital eccentricities, e_p, of which are 0.77, 0.52, and 0.0 (circular), for the dE,N with $R_{ini} = 200$ kpc in the FO model. Instead of R_{ini} and f_v, the orbital eccentricity (e_p), the apocenter (R_a), and the pericenter (R_p) of the orbit of a dE,N are used for describing the parameter set of the model, because these quantities are more informative.

The adopted value of 200 kpc for R_a (R_{ini}) in the fiducial model corresponds roughly to the projected distance of the observed most distant UCD from the center of the Fornax cluster (Drinkwater et al. 2000a, b). It takes $4-5$ Gyr for dE,Ns with $R_a = 200$ kpc to be transformed into UCDs, as is described later. The time scale for morphological transformation from dE,Ns into UCDs is longer for larger values of R_a (Bekki et al. 2001). Therefore, we investigate ~ 4.5 Gyr evolution of a dE,N for *all* models in order to draw robust conclusions as to whether the strong tidal field of the Fornax cluster can be responsible for UCD formation. Since UCDs can not be disintegrated after their formation for a reasonable set of parameters for galactic nuclei in dE,Ns (Bekki et al. 2001), we do not intend to investigate long-term (~ 10 Gyr) evolution of dE,Ns.

2.5 Choice of parameters

M_B and e_p are the most important parameters in determining whether a dE,N can be morphologically transformed into a UCD by galaxy threshing (Bekki et al. 2001); we therefore focus in most detail on the dependences our results have on these two parameters. The model that shows the typical behaviour of the galaxy threshing process, and is thus the most important in this study, is referred to as "the fiducial model" (FO1). This model has $M_B =$-16 mag, $a_n/a_{dw} = 0.02$, $M_n/M_{dw} = 0.05$, an SB dark matter profile with $e_p = 0.77$, $R_a = 200$ kpc, and the FO profile. By changing cluster mass profiles, host morphological types, dE,N luminosities, the dark matter profiles of the dE,Ns (as parameterised by a_n/a_{dw}, M_n/M_{dw}, e_p, and R_a), we investigate the parameter dependences of the galaxy threshing processes.

The parameter values and final morphologies for each model are summarized in the Table 1. In the first column, FO, VI, and LG represent the models with the Fornax cluster, Virgo cluster and Local Group mass profiles, respectively. Column 8 describes the final morphological properties of the dE,Ns and dwarf spirals after 4.5 Gyr orbital evolution. Here, "UCD" indicates a remnant whose envelope has been nearly completely stripped and yet whose nucleus remains largely unaffected (at most $\sim$ 20 % of the mass is stripped away); "dE,N" indicates the case where both the envelope and nucleus survive; "no remnant" indicates the case where both components are tidally stripped; and "UCD+LSB env" indicates a remnant that is dominated by the central compact nucleus yet has a non-negligible fraction (more than 5% of the total remnant mass) of the stellar envelope surrounding the nucleus.

Even if the envelopes of dE,Ns are nearly completely removed by galaxy threshing, not all of the threshed remnants can be identified as UCDs. The most extreme case is the F07 model where both the envelope and the nucleus of the dE,N are completely destroyed (and hence the "no remnant" classification in Table 1). In this model, $a_{\rm n}/a_{\rm dw}$ is rather large (0.2) and the nucleus is initially less compact and more susceptible to tidal destruction by a cluster tidal field. The dE,Ns with larger $a_{\rm n}/a_{\rm dw}$ (> 0.2) are less likely to be transformed into UCDs because of the lower degree of self-gravitation of the nuclei. Although such complete destruction of dE,Ns is very important in the context of the origin of the intracluster stellar light, we do not present here a detailed description of such "no remnant' models.

Finally, all the simulations have been carried out using GRAPE boards (Sugimoto et al. 1990) in the GRAPE 3 systems at Tohoku University and the GRAPE 5 systems at the National Astronomical Observatory in Japan. The total number of particles used for each model are 20,000 for the dark matter, 20,000 for the stellar envelope, and 10,000 for the nucleus. Multiple softening lengths are used for investigating the dynamical evolution of the three collisionless components with different size and mass. For each component (e.g., nucleus), the gravitational softening length is chosen such that the length is the same as the mean particle separation at the half-mass radius of the component. The time integration of the equation of motion is performed by using a second-order, leap-frog method. Most of the calculations are set to be stopped at $T = 4.5$ Gyr (corresponding to 20,000 time steps), where T represents the time that has elapsed since the simulation starts.

3   RESULTS

3.1   Fiducial model

Figures 1 and 2 summarise the dynamical evolution of the fiducial model and the morphological properties of the remnant in the model, respectively. As the dE,N approaches the pericenter of its orbit, the strong global tidal field of the Fornax cluster stretches the envelope of the dE'N along the direction of the dwarf's orbit and consequently tidally strips the stars of the envelope ($T = 1.13$ Gyr). The dark matter halo, which is more widely distributed than the envelope due to its larger core radius, is also efficiently removed from the
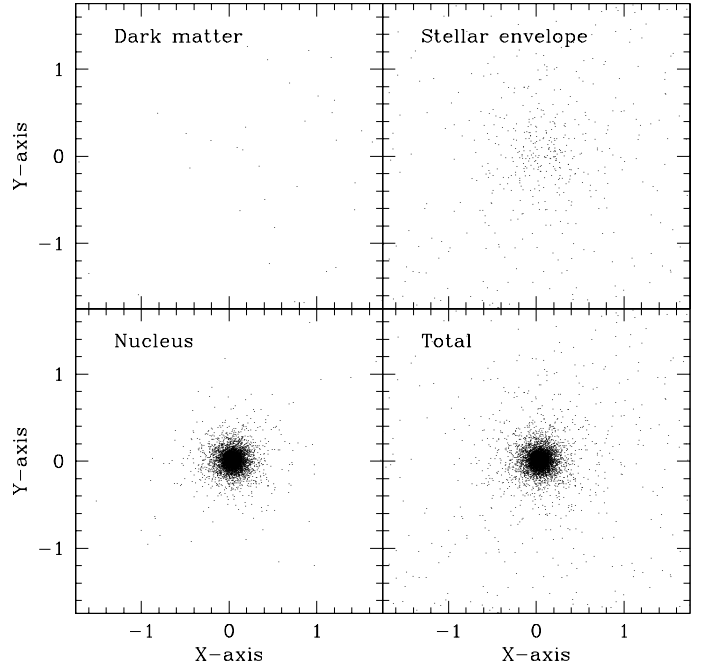

Figure 2. Final mass distributions projected onto the x-y plane at $T = 4.5$ Gyr for the dark matter halo (*upper left*), the stellar envelope (*upper right*), the nucleus (*lower left*), and all the components (*lower right*). The scale is given in units of kpc, and accordingly each frame measures 3.5 kpc on a side.

dE,N during the pericenter passage. Since the envelope (and the dark matter halo) loses a significant fraction of its mass during the passage of the pericenter, the envelope becomes more susceptible to the tidal effects of the Fornax cluster after the pericenter passage. Therefore, each subsequent time the dwarf approaches the pericenter, it loses an increasingly larger fraction of its stellar envelope through tidal stripping (compare, for example, the $T = 2.26$ and $T = 2.83$ Gyr time points). Consequently, both the envelope and the dark matter halo become smaller, less massive, and more diffuse after five passages of the pericenter ($T = 3.34$ Gyr).

The stripped stars form a long tidal stream along the "rosette" orbit within the orbital plane ($T = 1.13$ Gyr). The length and shape of the stream depend not only on the time T (the time that has elapsed since the simulation starts) but also on where the dE,N is located with respect to the center of the Fornax cluster. After a few pericenter passages, the stream comes to have the outer sharp edge at the apocenter of the dE's orbit ($T = 2.83$, 3.34, and 4.52 Gyr). Due to the longer time scale for the dynamical relaxation of stars in the tidal stream, the stars cannot be randomly dispersed into the intracluster region. Consequently, the finer stream can still be clearly seen after 4.5 Gyrs evolution of the dE,N. The developed stream is one of the observable predictions from the galaxy threshing model of UCD formation, and thus the existence or non-existence of such a stream extending from an UCD should be investigated observationally. Furthermore, the shape of the stream might well enable us to infer the orbit of the dE,N.
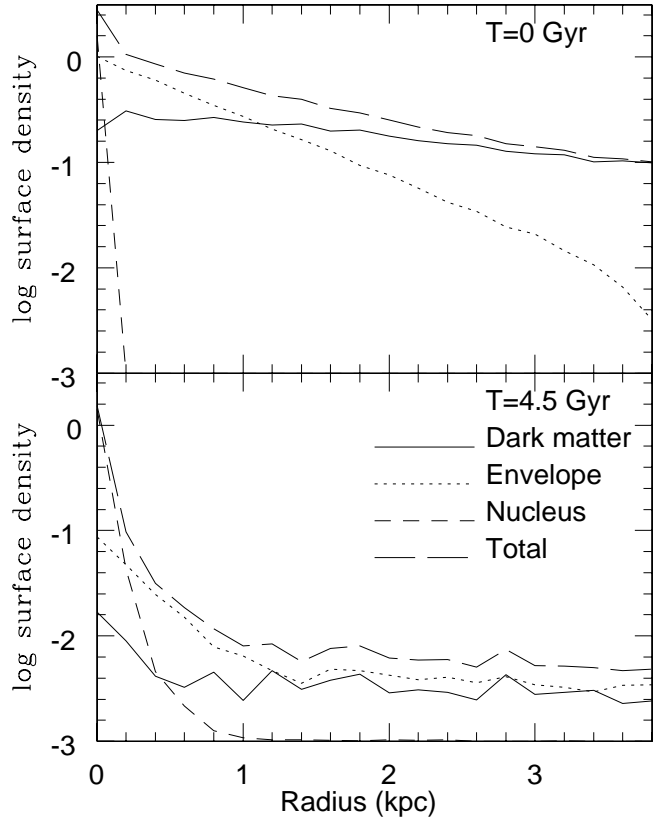
The central nucleus, on the other hand, is just weakly influenced by the tidal force as a result of its compact configuration. Because of its strongly self-gravitating nature,
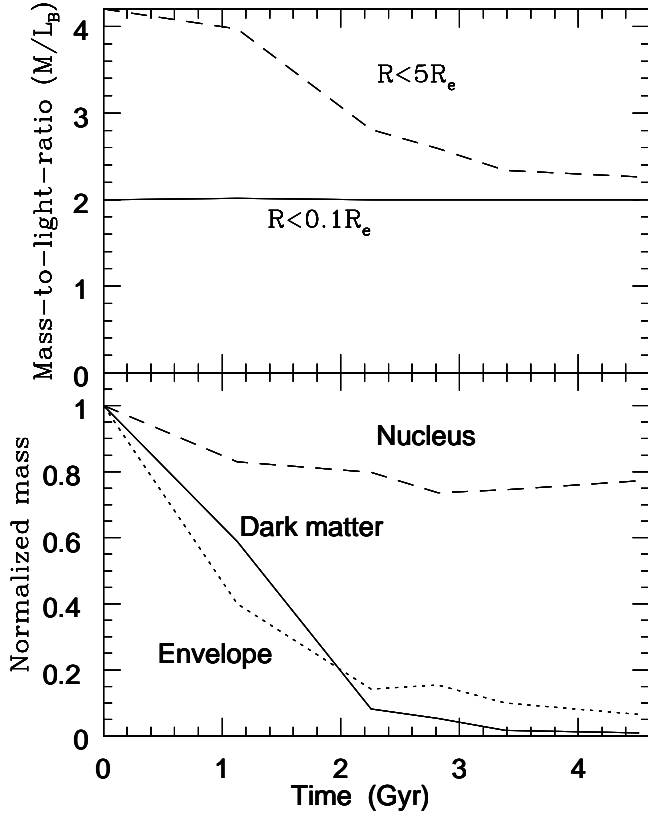
Figure 3. Time evolution of the B–band mass-to-light-ratio (M/L_{B}) (*upper* panel) and that of the total mass normalized to the initial mass for each collisionless component (*lower* panel) in the fiducial model (FO1). In the *upper* panel, M/L_{B} estimated for $R < 0.1R_{\mathrm{e}}$ (where R and R_{e} are the distance from the center of the dE,N and the initial effective radius of the dE,N, respectively) and for $5R_{\mathrm{e}}$, are shown by the *solid* and *dotted* lines, respectively. In the *lower* panel, the total mass within $R < 5R_{\mathrm{e}}$, $R < R_{\mathrm{e}}$, and $R < 0.1R_{\mathrm{e}}$ for the dark matter halo, the stellar envelope, and the nucleus is shown by the *solid, dotted* and *dashed* lines, respectively.

Figure 4. The projected surface density profiles for the dark matter (*solid* line), the stellar envelope (*dotted* line), the nucleus (*short-dashed* line), and all these components (*long-dashed* line) at $T = 0\,\mathrm{Gyr}$ (*upper* panel) and $4.5\,\mathrm{Gyr}$ (*lower* panel) in the fiducial model (FO1).

the nucleus loses only a small amount ($\sim 20\%$) of its mass and thus maintains its compact morphology during its tidal interaction with the Fornax cluster. As a result, a very compact stellar system with a negligible amount of dark matter is formed from the dE,N by $T = 4.5\,\mathrm{Gyr}$ (see Fig. 2). The total mass and size of the remnant are $\sim 3.8 \times 10^6\,M_\odot$ and $\sim 100\,\mathrm{pc}$ (five times the core or scale radius), consistent with the observed properties of a UCD. Hence this new study, based on fully self-consistent numerical models of dE,Ns, confirms the earlier results of Bekki et al. (2001b) based on a more simplistic model.

Figure 3 shows that the mass-to-light ratio, M/L_{B}, decreases dramatically from 4.2 to 2.3 for $r < 5r_{\mathrm{e}}$. This result clearly explains why the UCDs are observed to have mass-to-light ratios that are much smaller ($M/L_{\mathrm{B}} = 2\text{–}4$; D03) than those observed for dE,Ns (~ 10) for some of the Local group dwarf (van den Bergh 2000): galaxy threshing is the most efficient in the outer regions of a dE,N where the dark matter halo dominates gravitationally. About 95% of the envelope initially within r_{e}, and 20% of the nucleus initially within $0.1r_{\mathrm{e}}$ are removed from the dE,N. Figure 3 also suggests that a dE,N whose envelope has been par-

tially removed (i.e., at time $T = 2.83\,\mathrm{Gyr}$) has a smaller M/L_{B} and a larger $M_{\mathrm{n}}/M_{\mathrm{dw}}$ compared with the initial values. This implies that *if dE,Ns in a cluster are suffering from galaxy threshing, dE,Ns with smaller M/L_{B} are likely to show larger $M_{\mathrm{n}}/M_{\mathrm{dw}}$*. This possible correlation may well be observed thus providing a further test of the threshing scenario.

Figure 4 describes the final projected density profile of a UCD formed by galaxy threshing. Both the surface density of the dark matter and that of the envelope drop by more than an order of magnitude within $4.5\,\mathrm{Gyr}$. If the initial central surface brightness of the dE,N is $\mu_B = 23\,\mathrm{mag\,arcsec}^{-2}$, then the final surface brightness of the dE,N at $5a_{\mathrm{dw}}$ is about $\mu_B = 29\,\mathrm{mag\,arcsec}^{-2}$. Such a faint, low surface brightness envelope will be hard to detect, even by existing large ground-based telescopes. Thus the UCD formed by galaxy threshing shows a very steep density profile with an extremely low density outer "halo" ($R > 100\,\mathrm{pc}$) dominated by the original envelope component of the progenitor dE,N. This "halo" component surrounding a UCD is another important prediction of the threshing model. Furthermore, the total mass (or luminosity) and the surface brightness of this faint outer "halo" component are continually reduced as the threshing process proceeds to completion.

Figure 5 shows the location of the remnant of the fiducial model on the $[\sigma_0, M_{\mathrm{V}}]$–plane. In estimating M_{V} from the total mass of the remnant and the dE,N's initial values
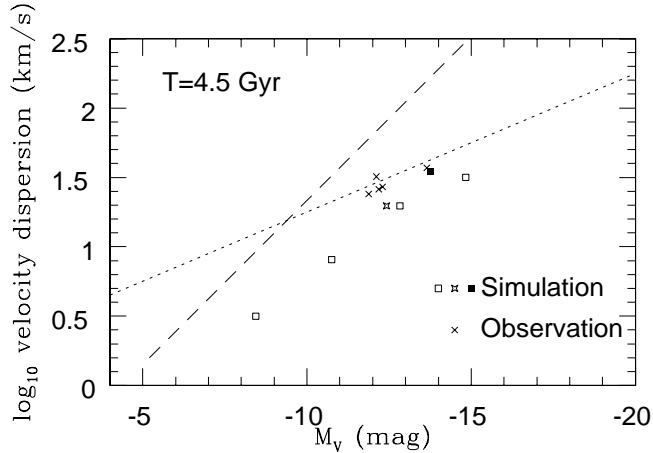
Figure 5. The distribution of the simulated UCDs on the [central velocity dispersion, M_V]–plane. Here we estimate M_V from the total stellar mass within $0.1R_e$ of the UCD formed by galaxy threshing, by assuming that the initial stellar nucleus has $M/L_B = 2$ and B-$V = 0.9$ (or 0.5). The mass ratio of the nuclear component to the envelope one is 0.05 for all models here. The central velocity dispersion is expressed in units of km s^{-1} but plotted on a $\log_{10}$ scale. The simulated UCDs are represented by *squares* (open, filled, and starred); the 5 UCDs observed by D03 are plotted (as *crosses*) for comparison. The *open* squares represent UCDs formed from dE,Ns with $M_B = -12, -14, -16$, and -18 mag. The brighter UCDs originate from brighter dE,Ns, and accordingly the *open* square at $M_V = -12.8$ mag is the UCD formed in the fiducial model with $M_B = -16$ mag. The *filled* square represents a UCD formed from a dE,N with $M_B = -16$ and a more massive nucleus ($M_n/M_{dw} = 0.2$). The *starred* square represents a UCD with $M_B = -16$ and $B - V = 0.5$. Long and short dashed lines represent the GC scaling relation (e.g., Djorgovski 1993) and Faber-Jackson one (1976), respectively.

of M_B and M/L_B, we assume that the B-V color of the remnant is 0.9 (also 0.5) mag, which is the same as the color D03 observed for their sample of UCDs. We estimate the central velocity dispersion from stars within 100 pc of the remnant of the threshed dE,N in each model. As is shown in this Figure, the remnant of the fiducial model has $M_V = -12.8$ mag (and $M_B = -11.9$), which is ~ 4 mag fainter than the initial dE,N, and $\log_{10}\sigma_0 = 1.3$, so that the location on the [σ_0, M_V]–plane is fairly close to that observed for UCDs. Figure 5 also demonstrates that: (i) only luminous dE,Ns ($M_B < -16$ mag) can become UCDs with $M_V < -12$ mag and $\sigma_0 > 20$ km s^{-2} after being threshed, (ii) the remnants of dE,Ns with the more massive (or bluer) nuclei lie closest to the location of the observed UCDs, and (iii) dE,Ns which overall are more luminous, are likely to become more luminous UCDs (if nuclear mass fraction is constant for dE,N populations) . The results shown in Figures 3, 4, and 5 thus confirm that galaxy threshing can transform *bright* dE,Ns (with the initial $M_B \sim -16$ mag) into compact stellar remnants with the structure and the kinematics similar to those observed in UCDs.

Figure 5 also implies that the UCDs observed by Drinkwater et al. (2000a, b), which have $M_V < -12$, must have had bright dE,N progenitors (with $M_B \sim -16$ mag) if they were transformed into UCDs by galaxy threshing. It also demonstrates that there can exist very compact objects with $M_V > -12$ mag (thus with M_B of the host dwarfs $>$

-16 mag) that do not lie on the GC scaling relation However, in the absence of kinematical information, such objects could easily be misidentified as GCs. Thus future central velocity dispersion measurements of the GC populations (identified around cluster galaxies via recession velocity measurements alone) may well uncover such a population of lower luminosity UCDs, distinguishable by their displacement from the GC scaling relation.

3.2 Parameter dependence

The physical properties of the threshed remnants depend strongly on the initial parameters of the progenitor galaxies and their orbits; these can be seen graphically in Figure 6. We find the following:

(i) UCDs can be formed by threshing only if the orbits of the progenitor dE,Ns are highly eccentric (e.g., $e_p > 0.7$ for $R_a = 200$ kpc and the FO profile). UCDs are more likely to be formed for dE,Ns orbiting the inner region of a cluster for a given e_p. These rather restrictive conditions would imply that UCD formation via galaxy threshing is expected to be a relatively rare event in clusters.

(ii) If the dark matter halos of dE,Ns have the central 'cuspy' cores that recent high-resolution simulations based on CDM models predict (e.g., NFW), these dE,Ns are less likely to be transformed into UCDs owing to the high central dark matter density. Conversely, if the observed UCDs really are threshed dE,Ns, the dark matter halos of the progenitor dE,Ns must have a 'softer' SB-like profile rather than an NFW-like profile. Final objects of dE,Ns with more compact dark matter halos have larger M/L_B because of a less amount of the stripped envelopes and the dark matter halos. These results suggest that dE,Ns observed in the central regions of the present-day clusters should have more compact dark matter halos to survive from galaxy threshing.

(iii) Galaxy threshing can transform nucleated dwarf spirals into UCDs, provided their central surface brightness (μ_0) is rather low ($\mu_0 \sim 26$ mag arcsec^{-2}). If the tidal field of a cluster is not strong enough to transform nucleated dwarf spirals into UCDs, it can transform them into nucleated S0-like objects due to the tidal heating of the stellar disks. High surface brightness nucleated spirals are very hard to be transformed into UCDs, even if the pericenter of the orbits is ~ 30 kpc.

(iv) UCD formation via dE,N galaxy threshing is more highly favoured in more massive clusters as a result of the stronger tidal field at a given radius from the cluster center. For UCDs to be formed in a small group like the Local Group while orbiting say our Galaxy, the pericenter of the dE,N's orbit should be ~ 5 kpc for $R_a = 50$ kpc (11 kpc for $R_a = 100$ kpc). This result implies that if UCDs exist around a luminous galaxy (like the Galaxy and M31), the pericenter of the orbits is likely to be within the optical radius of the galaxy (~ 20 kpc). This result provides some clue as to the origin of giant globular clusters such as ωCen and G1, which are located in the Local Group and could belong to the same class of compact object as UCDs.
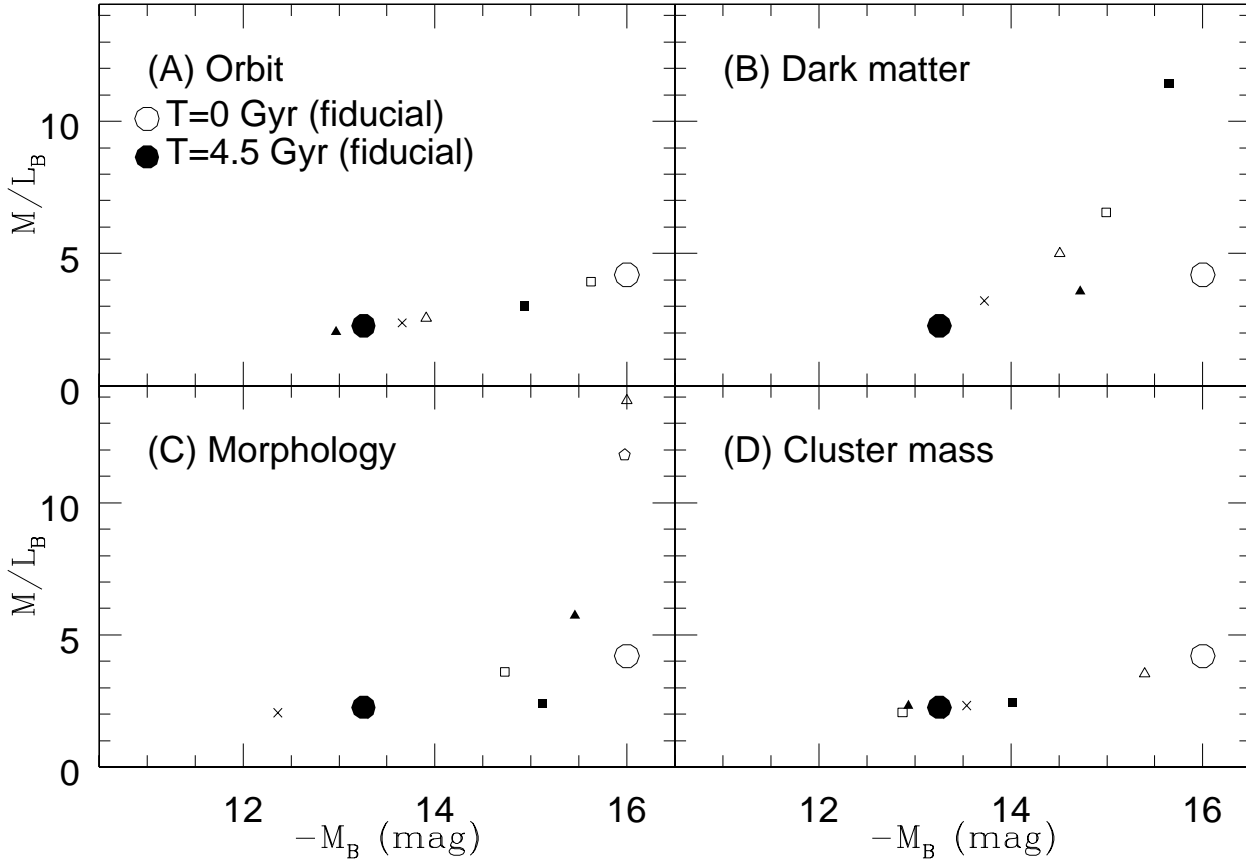
Figure 6. Distribution of 21 models with different parameter values on the $[M/L_B, M_B]$–plane. For all models, M_B and M/L_B are estimated for $R < 5R_e$. In all four frames, the results of the fiducial model at $T = 0$ Gyr (*open circle*) and 4.5 Gyr (*filled circle*) are plotted for comparison. *Upper left panel* (A): dependences on orbits for the FO7 (open triangles), FO8 (filled triangles), FO9 (open squares), FO10 (crosses), and FO11(filled squares) models. *Upper right panel* (B): dependences on the dark matter profiles for the F12 (open triangles), F13 (filled triangles), F14 (open squares), F15 (crosses), and FO16 (filled squares) models. *Lower left panel* (C): Dependences on host morphological types for the F17 (open triangles), F18 (filled triangles), F19 (open squares), F20 (crosses), F21 (filled squares), and F22 (open pentagons) models. *Lower right panel* (D): Dependences on cluster masses for the LG1 (open triangles), LG2 (filled triangles), VI1 (open squares), LG3 (crosses), and VI2 (filled squares) models . The parameter values for each model are given in Table 1. The M/L_B is estimated at $T = 4.5$ Gyr for the models. Note that the brighter remnants show higher M/L_B.

4   DISCUSSION

4.1   Predictions on total numbers and radial distributions of UCDs in clusters

Photometric and spectroscopic observations to search for UCDs in other nearby clusters (e.g., Virgo and Coma) are now ongoing (D03). The goal of these observational studies is to provide detailed information on (i) the physical properties of UCDs (e.g., total number, radial distribution, and luminosity function) in clusters, and (ii) the environmental dependence of these physical properties (e.g., Gregg et al. 2003). If these observations can be compared with the corresponding theoretical predictions of the galaxy threshing model, the plausibility of the model can be checked in a more self-consistent way. To aid this process, we use our models to generate predictions of the total number of UCDs and their radial distribution as a function of cluster mass.

First we derive the "threshing radius", R_{th}, within which the stellar envelope of a nucleated dwarf can almost entirely be removed by the strong tidal field of a cluster. R_{th} is different for dwarfs with different M_B in a given clus-

ter gravitational potential because of the observed mass-dependent density profiles of dark matter halos (Salucci & Burkert 2000). We estimate R_{th} for a dwarf orbiting a cluster by assuming that R_{th} is the distance from the cluster centre at which the tidal force of the cluster is equivalent to the self-gravitational force of the dwarf at the core radius of its dark matter halo. To be more specific, R_{th} for a dwarf with M_B satisfies the following relationship:

$$R_{th} = 2a_{dm}\left(\frac{M_{cl}(R_{th})}{M_{dm}}\right)^{1/3}, \tag{7}$$

where a_{dm}, $M_{cl}(R_{th})$, and M_{dm} are the dark matter core radius, the total mass of the cluster within R_{th}, and the total mass of the dark matter in the dwarf, respectively. Assuming the constant M/L_B (=10) adopted in the present study, we can estimate R_{th} numerically for dwarfs with a given M_B.

By assuming a cluster has a particular (i) mass-to-light-ratio (M/L), (ii) luminosity function, and (iii)a radial profile (for its galaxies and dark matter halo), we can also derive the spatial distribution and kinematics of galaxies in the cluster. We investigate here two cluster models: The "Fornax cluster
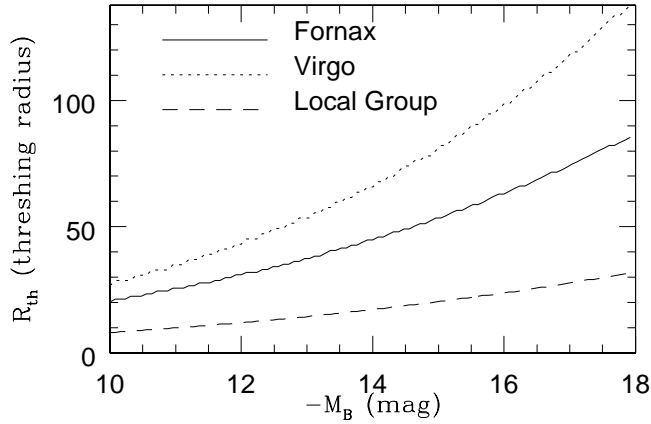
Figure 7. The dependence of the "threshing radius", $R_{\rm th}$ (in units of kpc), on $M_{\rm B}$ for our three cluster (group) models: "Fornax" (*solid* line), "Virgo" (*dotted* line), and "Local Group" (*dashed* line). A dE,N orbiting a cluster is considered to be transformed into a UCD (or a smaller compact stellar system) if the pericenter of the orbit is less than $R_{\rm th}$. An SB profile is adopted for the dE,N's dark matter component. The details of the three cluster models are given in the main text.
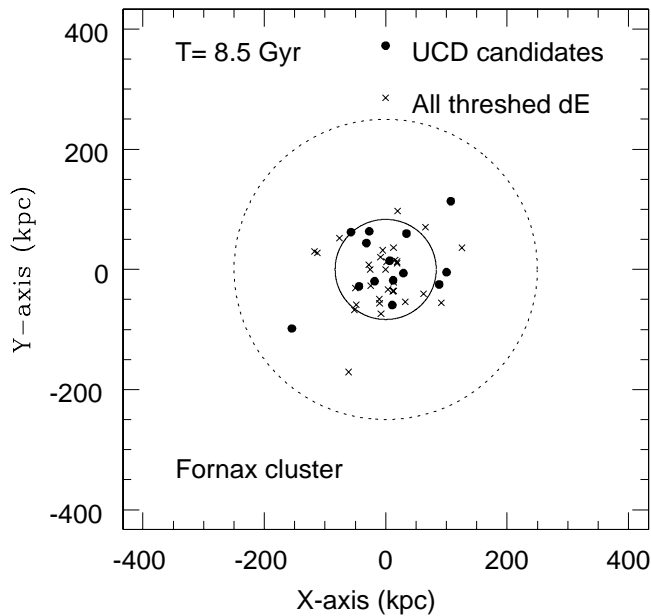

Figure 8. The projected distribution of UCDs (*filled* circles) and other threshed dEs (*crosses*) in the Fornax model. The *solid* and the *dotted* lines represent $r_{\rm s}$ (the cluster scale radius of the NFW profile) and $3r_{\rm s}$, respectively. The "UCD candidates" are threshed dE,Ns with $M_{\rm B} <$-16 mag, whereas the "all threshed dE" are threshed objects with $M_{\rm B} \geq$-16 mag. This distribution is derived after 8.5 Gyr of dE,N orbital evolution.

model" with total mass ($M_{\rm cl}$) of $7.0 \times 10^{13}\ M_\odot$ and $M/L = 200$, and the "Virgo cluster model" with $M_{\rm cl} = 5.0 \times 10^{14}\ M_\odot$ and $M/L = 500$. For comparison, we also investigate $R_{\rm th}$ for "the Local Group model" with $M_{\rm cl} = 3.0 \times 10^{12}\ M_\odot$ and $M/L = 100$. We adopt the Schechter function:

$$\Phi({\rm M}) = C_{\rm lf}\Phi^* 10^{0.4(\alpha+1)(M^*-M)}\exp(-10^{0.4(\alpha+1)(M^*-M)}), (8)$$

where Φ^*, α, and M^* are the number density, faint-end
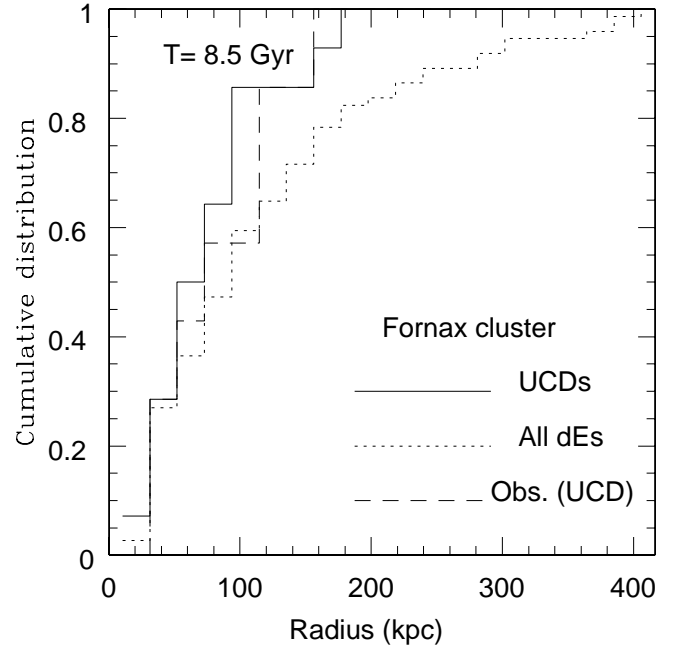
Figure 9. Cumulative radial distribution of UCDs (*solid* line) and all (initial) dwarfs with $-18 \leq M_{\rm B} \leq -10$ (*dotted* line) in the Fornax cluster model at $T = 8.5\ {\rm Gyr}$. For comparison, the observed distribution of UCDs (Drinkwater et al. 2000a, b) is shown by a dashed line. Note that UCDs are more centrally concentrated than dwarfs.

slope, and characteristic absolute magnitude quantities. We adopt the most recent observationally-determined values for these quantities: For α and M^* these are -1.07 and -19.7, respectively, as measured in the B-band by Efstathiou et al. (1988). The value of Φ^* is chosen according to the values of $M_{\rm cl}$ and M/L adopted for our model cluster. For the radial galaxy number distribution of galaxies in a cluster, we adopt a King profile with a core radius ~ 0.6 times smaller than the cluster scale radius, $r_{\rm s}$, in each cluster model (Adami et al. 1998). The value of $r_{\rm s}$ for each cluster model is chosen according to the simulated values of $r_{\rm s}$ in Table (e.g., model 15) of NFW.

Finally, we calculate, numerically, the orbit of each galaxy (represented by a test collisionless particle) moving within the cluster's gravitational potential, tracking it for 8.5 Gyr and thereby checking whether the galaxy comes within the threshing radius $R_{\rm th}$. In this calculation, we assume that the mean orbital eccentricity of galaxies in a cluster is 0.6, which is consistent with recent high-resolution cosmological simulations (Ghigna et al. 1998). We choose 8.5 Gyr rather than 4.5 Gyr in order to track evolution of dwarfs in clusters/group, because we need to check whether or not the dE,Ns with the apocenter distances larger than 200 kpc (corresponding to the distance of the most distant UCD from the center of the Fornax cluster) can be transformed into UCDs. Since we have found that $e_{\rm p}$ should be as large as 0.7 for outer dE,Ns to be transformed into UCDs, the predicted mean value of 0.6 in the CDM simulations (Ghigna et al. 1998) implies that UCD formation is not so common in clusters.

The host dwarfs of UCDs should be more luminous, because the observed mass fraction of nuclei in dE,Ns is less

than 0.2 (typically 0.02) and the UCDs are brighter than M_B < −11 mag. By adopting the observationally estimated stellar masses (an order of $10^7 M_\odot$) by D03, the stellar masses of UCD progenitor dE,Ns should be ∼ $10^9 M_\odot$, which corresponds to $M_B = −16$ mag for a reasonable mass-to-light-ratio of their stellar components. Given the absolute magnitude range observed for UCDs ($11 < −M_B \leq 13$), we take dwarf galaxies with $16 < −M_B \leq 18$ and a pericenter distance less than $R_{\rm th}$ to be the progenitors of UCDs. We thus investigate the total number and the radial distribution of UCDs in the two cluster models, based on our orbital calculations for galaxies of different absolute magnitude. Figure 7 describes the dependence of $R_{\rm th}$ on $−M_B$ for the two cluster models (as well as the Local Group). Irrespective of the cluster masses, $R_{\rm th}$ is smaller for less luminous galaxies.

Figure 8 shows the UCD distribution in the Fornax cluster model with $M_{\rm cl} = 7.0 \times 10^{13} M_\odot, M/L = 200$, and $r_s = 83$ kpc. In this model, 14 UCDs can be formed and all of them are within $3r_s$. This centrally concentrated UCD distribution is consistent with that observed by Drinkwater et al. (2000a, b), although note that the observations do not cover the full region shown in the Figure. How the UCDs are distributed spatially is further illustrated in Figure 9 where cumulative distributions are plotted. This clearly demonstrates that most of the UCDs are located within 200 kpc of the center of the Fornax cluster and that the UCDs are more centrally concentrated than the dwarf galaxy population. This is qualitatively consistent with the observations of Drinkwater et al. (2000a, b). Thus Figures 8 and 9 indicate the "truncation radius" within which UCDs can exist in a cluster. The derived number of 14 within 200 kpc is twice as much as the observed number of UCDs within 200 kpc pf the Fornax cluster.

In Figure 10 we show the UCD distribution in the Virgo cluster model, which has $M_{\rm cl} = 5.0 \times 10^{14} M_\odot, M/L = 500$, and $r_s = 226$ kpc. Most of the 46 UCD candidates are located within $3r_s$, which confirms that there is a "truncation radius" for UCDs in this cluster. As is shown in Figure 11, the cumulative distribution of UCDs in this model is qualitatively similar to that of the Fornax model. The total number of UCDs is larger and the UCDs are more widely distributed in the Virgo model than in the Fornax one. Thus these results predict that (i) the UCD distribution can be truncated at $R \sim 3r_s$, and (ii) the total number of UCDs is larger in more massive clusters. These predictions will be readily tested by future observations.

The total number of UCDs formed by galaxy threshing in the above simple simulation can depend on the total number of dE,Ns initially in a cluster thus on the luminosity function of galaxies in the cluster. Since the progenitor dwarfs of UCDs should be more luminous dE,Ns (typically $M_B \sim −16$), the simulated number of UCDs depends more strongly on the shape of the luminosity function around $M_B \sim −16$. Recently, Hilker et al. (2003) investigated the luminosity function of the Fornax cluster for fainter objects (with $M_V = −8.8$ mag) and found the faint-end slope of the luminosity function is flat ($\alpha \sim$ -1.1, See Pritchet & van den Bergh (1999) for the luminosity function of the Local Group of galaxies). These recent observational results are relevant to the number of dwarfs much fainter than UCD progenitor ones, so we think that adopting the most recent luminosity function does not change the above results so significantly.
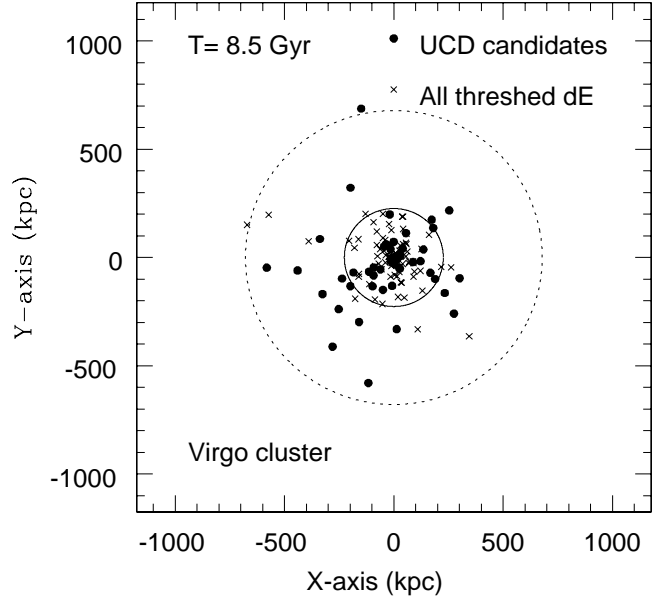

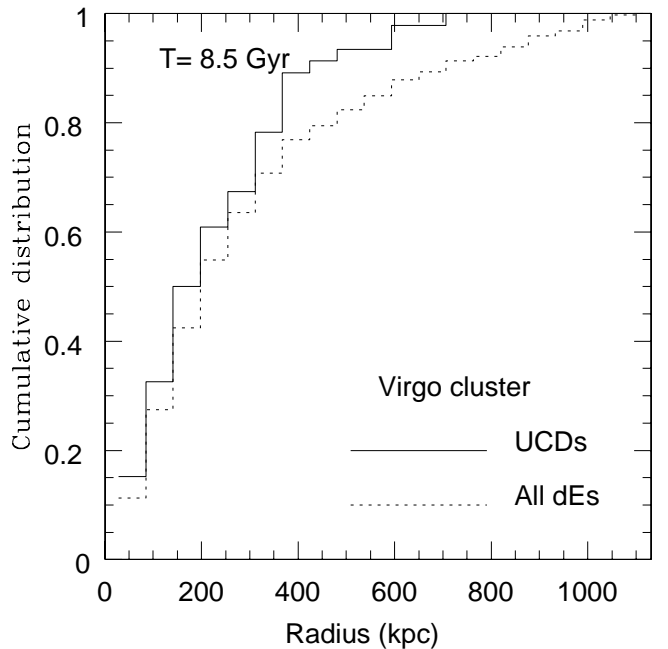**Figure 10.** As for Figure 8 but for the Virgo cluster model.

Figure 11. As for Figure 9 but for the Virgo cluster model.

4.2 Formation of stellar nuclei of dE,Ns through merging of star clusters

If UCDs can originate from the nuclei of nucleated dwarf galaxies, the next question is how these nuclei are formed within the cluster environment? Oh et al. (2000) first demonstrated that if the external tidal perturbation of a cluster of galaxies is relatively weak for a dwarf orbiting the cluster, dynamical friction can lead to significant orbital decay of the globular clusters within it and the formation of compact nuclei within a Hubble timescale. Fellhauer & Kroupa (2002) also showed that the merging of star clusters is essential to the formation of compact nuclei. One of the key
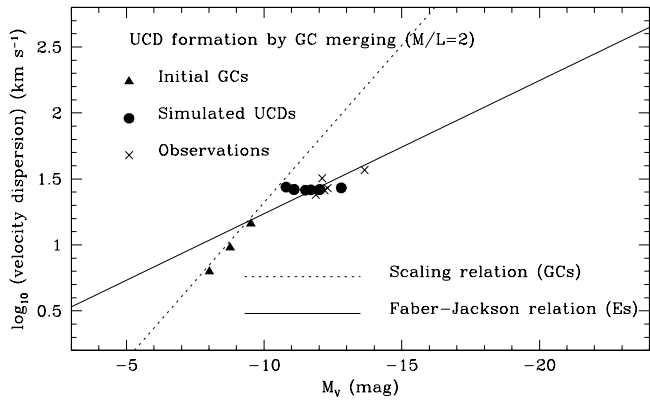
Figure 12. Distribution of UCDs formed from GC merging on the [central velocity dispersion, M_V]–plane. Six UCDs formed in the central regions of dEs via GC merging are represented by the *filled circles*. The central velocity dispersion is given in units of km s^{-1} and plotted on a log$_{10}$ scale. For comparison, the observed UCDs (*crosses*) and the original GCs (*filled triangles*) are also plotted. The *solid* and the *dotted* lines represent the scaling relations for GCs (Djorgovski 1993) and elliptical galaxies (Faber & Jackson 1976), respectively. The model and the method for deriving M_V and the central velocity dispersion of the UCDs formed from GC merging are given in the main text.

tests which can determine whether the above "merger scenario" of galactic nuclei formation is plausible and realistic is to investigate whether the scaling relations observed for UCDs (e.g., the Fundamental Plane [σ_0, M_B]– and [μ_0, M_B]–relations) are consistent with those of stellar systems formed by the merging of globular clusters.

Bekki et al. (2002a) investigated this point by comparing the results of numerical simulations of GC merging in dwarfs with the recent observations of D03. They found there to be consistent agreement between the scaling relations predicted for the simulated galactic nuclei and those observed for UCDs. Figure 12 briefly summarizes these results and demonstrates that the galactic nuclei formed by GC merging lie off the GC [σ_0, M_B]–relation and instead lie on or close to the Faber-Jackson relation, in the same region populated by the observed UCDs (see Bekki et al. 2002a, 2003 for details of the GC merger model). This result implies that conversion of the orbital angular momentum of the GCs into internal angular momentum of a single nuclear star cluster, and energy redistribution within the merging GCs, leads to a new scaling relation (upon which the UCDs lie) which is quite different to that defined by the GC population. Unfortunately, the lack of any observations which measure velocity dispersion profiles for UCDs makes it impossible to determine whether their kinematical properties are consistent with the GC merger scenario.

Clearly more extensive comparisons between the observed structural and kinematical properties of UCDs and the simulations are needed to determine whether their origin is in GC merging. Future high-resolution imaging of UCDs by HST/ACS will provide finer radial light distribution profiles and thus more precise estimates of their central surface brightness. These can then be compared with the observed (Kormendy 1984) and simulated versions of the [μ_0, M_B]–relation. Furthermore, the shapes of the simulated nuclei (or UCDs) in the GC merger scenario depends on the kinemat-

ics of the GC's host dwarf galaxy, such that dwarfs with more rotational energy (i.g., larger V/σ) are likely to have more flattened nuclei (Bekki et al. 2003). Therefore statistical studies of UCD shapes based on future high-resolution imaging will also provide a vital clue to the origin of galactic nuclei and UCDs.

4.3 Origin of higher M/L in UCDs

D03's study of the structure and kinematics of the UCDs in Fornax has revealed that their mass-to-light ratios range from 2 to 4 in solar units, based on the assumption that they are dynamically relaxed systems. These values are larger than the typical M/L of globular clusters ($M/L \sim 1$), and even larger than the largest globular clusters in M31 ($M/L = 1$-2). The most probable reason for this would be that UCDs are embedded by massive dark matter halos. However, the threshing scenario predicts that since nearly all of the dark matter can be tidally removed from dE,Ns in this process, the M/L of the formed UCDs should be as small as the M/L of the baryonic nuclei of the dE,Ns (Geha et al. 2002). Therefore, if UCD are formed by galaxy threshing, the dark matter halos should not be responsible for the higher M/L of UCDs (However, we here emphasize that if UCDs are *not* formed from galaxy threshing, the possibility of dark matter halos surrounding UCDs can not be ruled out).

Accordingly, if UCDs are formed by galaxy threshing and are predominantly baryonic, then the fact that their mass-to-light ratios are observed to be higher than the values typically measured for GCs suggests one of two possibilities: One is that the stellar populations of UCDs and GCs are quite different. The other is that the King model mass estimator, traditionally used for GCs (Meylan et al. 2001) but which has also been used to derive M/L values for UCDs (D03), is inapplicable to the latter because of fundamental differences in the structural and kinematical properties between UCDs and GCs.

With regard to the first possibility, we point out that the difference in the initial mass function (IMF) between UCDs and GCs is more likely to cause the observed difference in M/L between these two compact stellar systems Charlot et al. (1993) suggested that the IMF of stellar populations formed as the result of a starburst can be truncated, thus resulting in a higher M/L. Recent hydrodynamical simulations have demonstrated that star clusters rather than field stars are more likely to form in the central regions of interacting and merging galaxies with strong starbursts because the high pressure of the interstellar gas can trigger the collapse of giant molecular clouds (Bekki & Couch 2001; Bekki et al. 2002b). Oh et al. (2000) showed that star clusters can merge with one another to form a single nucleus in a dwarf galaxy because of the efficient dynamical friction of the clusters. Together these results imply that if compact nuclei are formed by the merging of young star clusters in starbursting dwarf galaxies, then they (and hence UCD progenitors) will have a higher M/L. Spectrophotometric studies which place strong constraints on the IMF of young star clusters in starbursting dwarf galaxies provide an important text of this first scenario.

With regard to the measurement of the mass-to-light ratio, we note that M/L is assumed to be proportional to

the product of r_e and σ_0 in the formula adopted by D03. Therefore the M/L of each UCD can be overestimated if either the effective radius (r_e) or the central velocity dispersion (σ_0) is overestimated for some observational reason. The possibility that r_e is overestimated by a factor of 2–4 is highly unlikely, because the observed radial profiles are fitted so well by either a King model or de Vaucouleurs ($R^{1/4}$) profile (D03). On the other hand, the velocity dispersion of a UCD is very likely to decrease with radius, like other self-gravitating systems such as elliptical galaxies. Because D03's spectroscopic observations were made through a slit that was large compared to the angular sizes of the UCDs, this would cause their central velocity dispersions to be underestimated, in the opposite direction to that required for an overestimation of M/L. Although other systematic observational effects cannot be ruled out entirely, it would seem more likely that the difference between the M/L for GCs and UCDs is real and related to differences in their stellar populations.

4.4 Physical relationship between UCDs and ωCen

The globular cluster ωCen is the most massive such system in our Galaxy and is observed to have unique physical properties such as a very broad metallicity distribution (Freeman & Rodgers 1975) and a highly flattened shape (Meylan 1987). These unique characteristics have been cited as evidence for ωCen having a very different star formation, chemical enrichment and structure formation history to other Galactic globular clusters (e.g., Majewski et al. 1999; Hilker & Richtler 2000). Such highly flattened, luminous globular clusters are also known to reside around M31, the most notable being G1 (Meylan et al. 2001), with another recently discovered by Larsen (2001).

One of the most extensively discussed formation scenarios for these giant GCs is that they are the surviving nuclei of ancient nucleated dwarfs in the Local Group of galaxies. Bekki & Freeman (2003) recently demonstrated that ωCen could have been formed from a nucleated dwarf as a result of its outer stellar envelope being completely tidally stripped by the Galaxy. The original nucleated dwarf would have had an absolute magnitude of $M_{\rm B} = -14$ and been in a retrograde orbit with respect to the Galaxy. Although there is nearly an order of magnitude difference in luminosity between UCDs and giant GCs such as ωCen and G1, both can be formed via the same 'threshing' mechanism. Thus it seems plausible to propose a theoretical model in which UCDs and giant globular clusters belong to the same family of objects with a common progenitor – the nuclei of dE,Ns, – but whose luminosities/sizes differ between these two classes.

There are, however, two apparent differences between UCDs and giant GCs. Firstly, both ωCen and G1 seem to lie on the GC $[M_{\rm B}, \sigma_0]$ scaling relation, whereas UCDs do not. Secondly, both ωCen and G1 are considerably flattened with flatness parameter (ϵ) values of 0.121 (Geyer et al. 1983) and 0.2 (Meylan et al. 2001), respectively. These values are much larger than the values typical of Galactic GCs ($\epsilon = 0.006$; White & Shawl 1987). There is no clear evidence that UCDs are as flattened as ωCen and G1 (D03), although the ability of *HST* imagery to precisely measure their flatness is rather limited. This difference would imply that *if both giant GCs and UCDs originate from dE,N nuclei, the less luminous dwarfs should have more flattened nuclei.* Future statistical studies (based on deep imaging at high spatial resolution) of whether there is a correlation between flatness and the luminosity of nuclei in dwarfs will provide a direct test of this model.

5 CONCLUSIONS

We have investigated, numerically, how the global tidal field of a cluster transforms dE,Ns morphologically into UCDs for a range of models with different cluster masses and sizes. We summarise our principle results as follows:

(1) For a plausible dwarf galaxy scaling relation, the outer stellar components of a dE,N orbiting a cluster is almost totally stripped as a result of the strong cluster tidal field; the nucleus, on the other hand, manages to survive. The naked nucleus developed in this 'galaxy threshing' process will be classified as a UCD (satisfying the same criteria by which UCDs were discovered in the Fornax cluster) providing its host was more luminous than $M_{\rm B} = -16$ mag. The mass-to-light-ratio of the threshed dE,N decreases dramatically from ~ 10 to ~ 2 during the course of several passages through the central region of the cluster.

(2) For a dE,N to be transformed into a UCD by threshing, its orbit needs to be highly eccentric. As an example, dE,Ns with flat dark matter cores must have orbital eccentricities of $e_{\rm p} > 0.7$ for $R_a \sim 200$ kpc and $e_{\rm p} > 0.4$ for $R_a = 100$ kpc in the Fornax model. This requirement does not depend on cluster mass.

(3) The initial dark matter density profile of the dE,N is critical in determining whether it is transformed into a UCD by the threshing process. dE,Ns embedded in dark matter halos with NFW profiles (i.e., 'cuspy' dark matter cores) are less likely to be transformed into UCDs, because their stellar envelopes are much more strongly bound. This implies that if UCDs are formed via galaxy threshing, the progenitor dE,Ns must have very flat, low-density dark matter cores.

(4) Nucleated dwarf spirals can also be transformed into UCDs, but only if they have a low central surface brightness ($\mu_0 \sim 26$ mag arcsec^{-2} in the B-band) and larger orbital eccentricities ($e_{\rm p} > 0.5$). Spirals with brighter central surface brightnesses ($\mu_0 \sim 24$ mag arcsec^{-2}) can instead be transformed into nucleated S0s as a result of the strong disk heating by the cluster's tidal field. High surface brightness nucleated dwarf spirals with $\mu_0 \sim 22$ mag arcsec^{-2} cannot be transformed into UCDs, even if they are on highly eccentric ($e_{\rm p} \sim 0.8$) orbits.

(5) UCDs are more likely to be formed in more massive clusters (or groups), because their stronger tidal fields makes the galaxy threshing process more efficient. The total number of UCDs formed by threshing is larger and the UCDs are more widely distributed in such clusters. Our threshing model predicts that there is a "truncation radius" within which UCDs can exist in a cluster.

6   ACKNOWLEDGMENT

REFERENCES

Adami, C., Mazure, A., Katgert, P., Biviano, A. 1998, A&A, 336, 63

Bassino, L. P., Muzzio, J. C., & Rabolli, M. 1994, ApJ, 431, 634

Bekki, K., Couch, W. J., 2001, ApJL, 557, 19

Bekki, K., Couch, W. J., Drinkwater, M. J., Gregg, M. D. 2001a, ApJL, 557, 39

Bekki, K., Couch, W. J., Drinkwater, M. J. 2001b, ApJL, 552, 105

Bekki, K., Couch, W. J., & Drinkwater, M. J. 2002a, in IAU 8th Asian-Pacific regional meeting, edited by S. Ikeuchi, J. Hearnshaw, & T. Hanawa, (PASJ), p 245.

Bekki, K., Forbes, D. A., Beasley, M. A., Couch, W. J. 2002b, MNRAS, 335, 1176

Bekki, K., Couch, W. J., & Drinkwater, M. J., Shioya, Y. 2003, in preparation

Bekki, K., Freeman, K. C. 2003, in preparation

Binggeli, B., Sandage, A., Tammann, G. A. 1985, AJ, 90, 1681

Binggeli, B., Cameron, L. M., 1991, A&A, 252, 27

Binney, J., Tremaine, S., 1987 in Galactic Dynamics.

Burkert, A. 1994, MNRAS, 266, 877

Burkert, A. 1995, ApJL, 447, 25

Charlot, S., Ferrari, F. Mathews, G. J., Silk, J. 1993, ApJL, 419, 57

Dirsch, B., Richtler, T., Geisler, D., Forte, J. C., Bassino, L. P., Gieren, W. P. 2003, AJ, 125, 1908

Djorgovski, S. 1993, in ASP Conf. Ser. 48 The globular cluster-galaxy connection. ed. Graeme H. Smith and Jean P. Brodie (San Francisco: ASP), p496

Drinkwater, M. J., Phillipps, S., Jones, J. B., Gregg, M. D., Deady, J. H., Davies, J. I., Parker, Q. A., Sadler, E. M., Smith, R. M. 2000a, A&A, 355, 900

Drinkwater, M. J., Jones, J. B., Gregg, M. D., Phillipps, S. 2000b, PASA, 17, 227

Drinkwater, M. J., Gregg, M. D., Colless, M. 2001, ApJL, 548, 139

Drinkwater, M. J., Gregg, M. D., Hilker, M., Bekki, K., Couch, W. J., Ferguson, J. B., Jones, J. B., Phillipps, S. 2003, Nature, in press (D03)

Efstathiou, G., Ellis, R. S., Peterson, B. A. 1988, MNRAS, 232, 431

Faber, S. M. 1973, ApJ, 179, 423

Faber, S. M., Jackson, R. E. 1976, ApJ, 204, 668

Fellhauer, M., Kroupa, P. 2002, MNRAS, 330, 642

Ferguson, H. C., Bingelli, B. 1994, A&ARv, 6, 67

Forbes, A. F., Beasley, M. A., Bekki, K. 2002, in Sky & Space, Aug/Sep 2002, p18

Freeman, K. C., Rodgers, A. W. 1975, ApJL, 201, 71

Freeman, k. C. 1993, in The globular clusters-galaxy connection, edited by Graeme H. Smith, and Jean P. Brodie, ASP conf. ser. 48, p608

Geha, M., Guhathakurta, P., van der Marel, R. P. 2002, AJ, 125, 3073

Ghigna, S., Moore, B., Governato, F., Lake, G., Quinn, T., Stadel, J. 1998, MNRAS, 300, 146

Geyer, E. H., Nelles, B., Hopp, U. 1983, A&A, 125, 359

Gregg, M. D., Drinkwater, M. J. 2003, in preparation

Harris, W. E., Pritchet, C. J., McClure, R. D., 1995, ApJ, 441, 120

Hilker, M., Infante, L., Richtler, T. 1999, A&AS, 138, 55

Hilker, M., Richtler, T. 2000, A&A, 362, 895

Hilker, M., Mieske, S., Infante, L. 2003, A&A, 397L, 9

Jones, C., Stern, C., Forman, W., Breen, J., David, L., Tucker, W., Franx, M. 1997, ApJ, 482, 143

King, I. R. 1962, AJ, 67, 471

Kormendy, J. 1977, ApJ, 218, 333

Larsen, S. S. 2001, AJ, 122, 1782

Lotz, J. M.; Telford, R., Ferguson, H. C., Miller, B. W., Stiavelli, M., Mack, J. 2001, ApJ, 552, 572

Majewski, S. R. et al 1999, The Galactic Halo : From Globular Cluster to Field Stars, Proceedings of the 35th Liege International Astrophysics Colloquium, Edited by A. Noels, P. Magain, D. Caro, E. Jehin, G. Parmentier, and A. A. Thoul. p619

Mateo, M. 1998, ARAA, 36, 435

Mateo, M., Olszewski, E., Welch, D. L., Fischer, P., Kunkel, W. 1991, AJ, 102, 914

Meylan, G. 1987, A&A, 184, 144

Meylan, G., Sarajedini, A., Jablonka, P., Djorgovski, S. G., Bridges, T., Rich, R. M. 2001, AJ, 122, 830

Mihos, J. C., McGaugh, S. S., de Blok, W. J. G. 1997, ApJL, 477, 79

Moore, B. 1994, Nature, 370, 629

Navarro, J. F., Frenk, C. S., White, S. D. M. 1996, ApJ, 462, 563

Nieto, J.-L., & Prugniel, P. 1987, A&A, 186, 30

Oh, K. S., Lin, D. N. C. 2000, ApJ, 543, 620

Pritchet, C. J., van den Bergh, S. 1997, AJ, 118, 883

Salucci, P., Burkert, A. 2000, ApJL, 537, 9

Sandage, A., Binggeli, B., Tammann, G. A. 1985, AJ, 90, 1759

Sugimoto, D., Chikada, Y., Makino, J., Ito, T., Ebisuzaki, T., Umemura, M. 1990, Nature, 345, 33

van den Bergh, S. 2000, The Galaxies of the Local Group (Cambridge University Press).

White, R. E., Shawl, S. J. 1987, ApJ, 317, 246

Zinnecker, H., Keable, C. J., Dunlop, J. S., Cannon, R. D., Griffiths, W. K. 1988, in Grindlay, J. E., Davis Philip A. G., eds, Globular cluster systems in Galaxies, Dordrecht, Kluwer, p603

Table 1. Model parameters and results of galaxy merging and interaction.

Model no.	host [a]	M_B (mag)	dark matter [b]	R_a (kpc)	R_p (kpc)	e_p	final morphology [c]	comments
FO1	dE,N	-16	SB	200	27	0.77	UCD	fiducial model
FO2	dE,N	-12	SB	200	27	0.77	UCD	
FO3	dE,N	-14	SB	200	27	0.77	UCD	
FO4	dE,N	-18	SB	200	27	0.77	UCD	
FO5	dE,N	-16	SB	200	27	0.77	UCD	$M_n/M_{dw} = 0.2$
FO6	dE,N	-16	SB	200	27	0.77	no remnant	$a_n/a_{dw} = 0.2$
FO7	dE,N	-16	SB	100	100	0.0	dE,N	
FO8	dE,N	-16	SB	100	35	0.48	UCD	
FO9	dE,N	-16	SB	200	200	0.0	dE,N	
FO10	dE,N	-16	SB	200	65	0.52	UCD+LSB env.	
FO11	dE,N	-16	SB	400	47	0.79	dE,N	
FO12	dE,N	-16	SB	200	27	0.77	dE,N	$a_{dm} = 0.5a_{dm,0}$
FO13	dE,N	-16	NFW	200	65	0.52	dE,N	$a_s = a_{dm,0}$
FO15	dE,N	-16	NFW	200	27	0.77	UCD+LSB env.	$a_s = a_{dm,0}$
FO14	dE,N	-16	NFW	200	27	0.77	dE,N	$a_s = 0.5a_{dm,0}$
FO16	dE,N	-16	NFW	200	27	0.77	dE,N	$a_s = 0.25a_{dm,0}$
FO17	Sp(HSB)	-16	SB	200	65	0.52	Sp	μ_0=22 mag arcsec^{-2}
FO18	Sp(LSBI)	-16	SB	200	65	0.52	S0	μ_0=24 mag arcsec^{-2}
FO19	Sp(LSBI)	-16	SB	200	27	0.77	UCD with LSB.env	μ_0=24 mag arcsec^{-2}
FO20	Sp(LSBII)	-16	SB	200	65	0.52	UCD	μ_0=26 mag arcsec^{-2}
FO21	Sp(LSBI)	-16	SB	200	65	0.52	S0	$a_{dm}/a_{disc} = 12$
FO22	Sp(HSB)	-16	SB	100	35	0.48	Sp/S0	
VI1	dE,N	-16	SB	200	27	0.77	UCD	
VI2	dE,N	-16	SB	400	58	0.75	UCD with LSB env.	
LG1	dE,N	-16	SB	200	21	0.81	dE,N	
LG2	dE,N	-16	SB	50	5	0.81	UCD	
LG3	dE,N	-16	SB	100	11	0.80	UCD	

[a] Morphological type of the host galaxy: dE,N, Sp, HSB, and LSB represent nucleated dwarf ellipticals, spirals, high surface brightness galaxies, and low surface brightness ones, respectively.
[b] SB and NFW represent the dark matter radial profiles by Salucci & Burkert (2000) and by Navarro, Frenk, & White (1995), respectively.
[c] UCD+LSB env. means the UCD embedded by very low surface brightness stellar envelope.

This figure "f1.copy.jpg" is available in "jpg" format from:

http://arXiv.org/ps/astro-ph/0308243v1